Progress In Electromagnetics Research C, Vol. 93, 253–263, 2019

A New RF MEMS Capacitive Switch for K-Band Application

Hao Wei[1, *], Shiwang Jia[1], Fei Zhao[1], Lanyuan Dang[1], Guanghua Liang[1], Yaxin Xu[1], and Zhongliang Deng[2]

Abstract—This paper proposes a novel RF MEMS capacitive shunt switch, which is applied in K-band ($18 \sim 26.5$ GHz). The characteristic impedance matching of the RF MEMS switch is achieved by discontinuous coplanar waveguide (DCPW) structure. Two actuation poles are located at the bottom of the fixed-fixed beam, and they are covered with a dielectric layer of SiN. The pole's thickness is less than that of CPW signal, to avoid the phenomenon of dielectric charging between the beam and the pole. The proposed MEMS switch is fabricated on 400 µm-thickness high resistivity silicon, using the MEMS surface micromachining process. Measured results demonstrate that, at K-band, the return loss is better than 22 dB, and the insertion loss and isolation are better than 0.5 and 17 dB, respectively. The on/off switched time is 168/54 µs when the DC bias voltage is 0/54 V. This proposed MEMS switch provides a solution for K-band communication system applications.

1. INTRODUCTION

With the rapid development of low earth obit (LEO) satellite constellations, phased array antenna is studied more and more [1]. Switch plays an important role in a phased array antenna, such as phased shifter [2, 3] and switching network [4]. MEMS process technology exhibits a high machining precision [5], compared with PIN switch and FET switch, and RF MEMS switch exhibits low insertion, low power consumption, and high isolation [6]. MEMS switch can be integrated with an antenna to achieve a reconfigurable pattern [7–9].

Many RF MEMS switches with high performances have been reported. Radant Corporation developed a series of RF MEMS switches products, such as RMSW101, RMSW101HP, RMSW201, and RMSW201HP. The performances of these switches products are very good. Recently, ADI Corporation has reported some RF MEMS switches product with excellent performance [10]. Topalli et al. [11] have designed some inductively tuned RF MEMS capacitive switches, but impendence matching properties of these switches in working frequency have never been achieved. However, the forms of these switches are all Omron DC contact switches, whose operating frequencies are from DC to Ku band because their isolation cannot be more than 20 dB. Higher frequency RF MEMS switches with good performance should be resolved urgently.

Many researchers have designed various RF MEMS switches, applied in K band, with a relatively low insertion loss and high isolation. Persano et al. [12] have proposed a K-band RF MEMS switch with electrostatic actuation, and the switch's measured switching time is 100 µs. However, the switch's S_{11} parameter has not been given, and the switch's structure is likely to cause dielectric charging. Cohn et al. [13] have designed a MEMS switch with a high lifetime, but the switching time is not measured. Yang et al. [14] have proposed a MEMS switch with fast switching time, and the pull-in/release switching time is 55/20 µs, respectively. However, the switch's insertion loss is nearly 1 dB, and the isolation is only

Received 24 March 2019, Accepted 23 June 2019, Scheduled 5 July 2019

* Corresponding author: Hao Wei (haowei@bupt.edu.cn).

[1] The 54th Research Institute of China Electronics Technology Group Corporation (CETC-54), Shijiazhuang 050051, China. [2] Beijing University of Posts and Telecommunications, Beijing 100876, China.

11 dB at 20 GHz. Bakri-Kassem and Mansour [15] have designed a low insertion loss MEMS switch with hot actuation, but the pull-in and release switching times of the switch are 14 and 3 ms, respectively. Carty et al. [16] have reported an RF MEMS with integrated driver circuitry applied in K band, but the switching time has not been given. Hamad et al. [17] have proposed a K band MEMS reconfigurable resonator using DGS structure, but only simulated the performance of the MEMS switch.

This paper designs, fabricates, measures, and analyzes a K-band RF MEMS capacitive switch. DCPW structure is applied in this MEMS switch to realize impedance matching at K band. Meanwhile, a new switch's structure is designed to resolve dielectric charging. The relationship among the beam, pole, and switching time is analyzed. The MEMS switch is fabricated on 400 μm high resistivity silicon, and the properties of the switch are measured. In K band, this proposed MEMS switch exhibits a good performance, and measured results match simulated ones very well.

2. DESIGN AND SIMULATION OF THE RF MEMS SWITCH

2.1. Mechanics Modeling and Structure Design of High Performance RF MEMS Beam

In the design of the MEMS capacitive shunt switch, the relationship among the actuation poles' topology, the spring constant of the fixed-fixed beam, and actuation voltage is researched firstly. The proposed switch in this paper uses two poles located at the ends, which is as illustrate in Fig. 1.

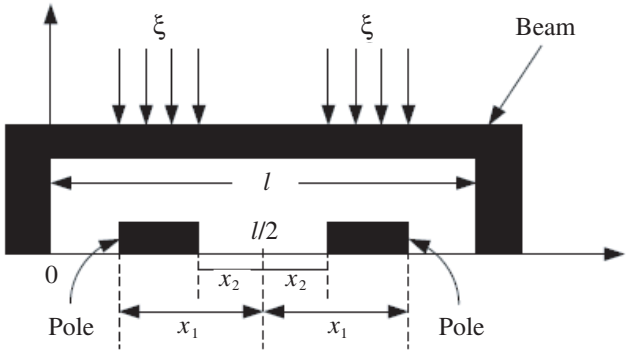

Figure 1. Fixed-fixed beam with the force evenly distributed along the ends of the beam [20].

The spring constant k, actuation voltage V, tspring constant k_1 caused by the beam's stiffness and the spring constant k_2 caused by the beam's residual stress are calculated from formulas (1) $\sim$ (7) [6].

$$k = k_1 + k_2 \tag{1}$$

$$V = \sqrt{\frac{8k}{27\varepsilon_0 (2w(x_1 - x_2))} g^3} \tag{2}$$

$$k_1 = -\frac{P}{\frac{2}{EI}\int_{\frac{l}{2}+x_1}^{\frac{l}{2}+x_2} \frac{\xi}{48}\left(l^3 - 6l^2a + 9la^2 - 4a^3\right) da} \tag{3}$$

$$k_2 = -\frac{P}{2\int_{\frac{l}{2}+x_1}^{\frac{l}{2}+x_2} \frac{\xi}{2S}(l-a)\, da} \tag{4}$$

$$S = \sigma(1-\upsilon)tw \tag{5}$$

$$I = \frac{wt^3}{12} \tag{6}$$

$$P = 2\xi (x_1 - x_2) \tag{7}$$

where ξ is the load per unit length, and P is the total load. Parameters of $I, l, w, t, \sigma, \nu, S, E$ and ε_0 represent the moment of inertia, length of the beam, width of the beam, thickness of the beam, biaxial residual stress, tensile force of biaxial residual stress, Poisson's ratio, Young's modulus, and permittivity of vacuum, respectively.

As illustrate in Fig. 2, the relationship among the pull-in voltage V_p, spring constant k, and poles'position (x_1 and x_2) is given. The spring constant increases with the increase of poles' area. The voltage decreases with the decrease of x_1's value and the increase of x_2's value. The minimum value of the voltage can be obtained in the range of x_1 and x_2.

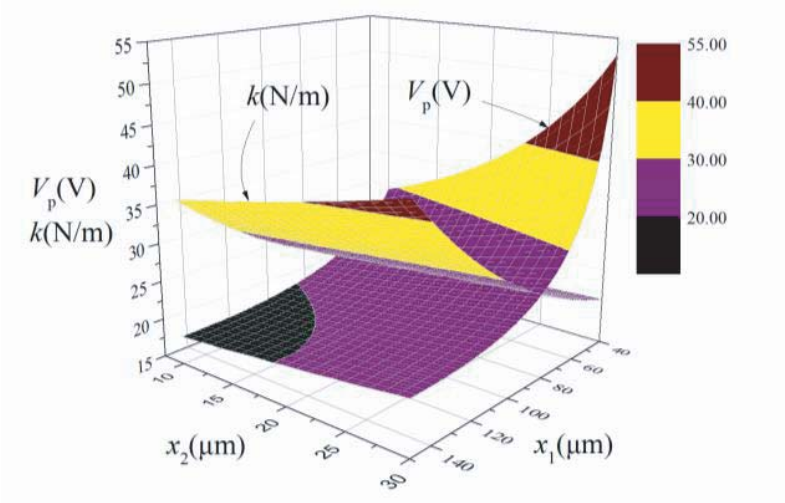

Figure 2. The relationship among the pull-in voltage V_p, the spring constant k and the poles'position (x_1 and x_2) [20].

For example, for the beam with a width of 100 μm, a length of 400 μm, thickness of 1 μm, gap of 1.5 μm, x_1 of 200 μm, and x_2 of 10 μm, the relationship among the pull-in voltage V_p, spring constant k, and residual stress σ is as shown in Fig. 3. The value of V_p increases obviously with the increase of the value of σ.

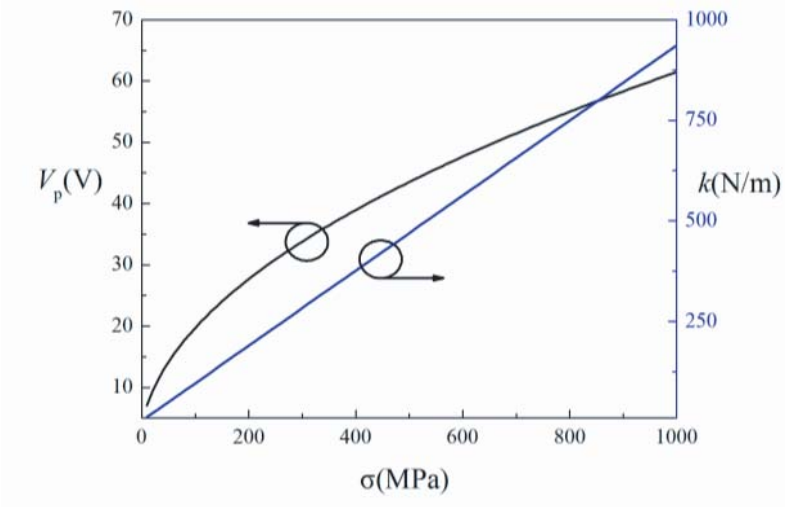

Figure 3. The relationship among the pull-in voltage V_p, the spring constant k and the residual stress σ [20].

The dynamic mechanical properties of the MEMS switch can be analyzed as follow [6].

$$\frac{1}{2}mv^2 = \frac{1}{2}kg^2 - \frac{1}{2}kx^2 \tag{8}$$

where parameters of x, v, m, k, and g represent the displacement, pull-in speed, mass, spring constant, and initial gap of the MEMS beam, respectively. The switching time can be given by Eqs. (9) $\sim$ (10) [6].

$$v = \sqrt{\frac{kg^2 - kx^2}{m}} \tag{9}$$

$$t_s = \int_0^g \frac{dx}{v} = \sqrt{\frac{m}{k}} \int_0^g \sqrt{\frac{1}{g^2 - x^2}} dx = \left[\sqrt{\frac{m}{k}} \arcsin \frac{x}{g}\right]_0^g = \frac{\pi}{2}\sqrt{\frac{m}{k}} = \frac{\pi}{2\omega_0} \tag{10}$$

In order to research the relationship between the actuation voltage and switching time, the relationship among the thickness, spring constant, and switching time is analyzed. When x_1 is 50 μm, the width of beam is 100 μm, the gap 1.5 μm, and residual stress 10 MPa. The calculated results from above formulas are described as shown in Fig. 4. To improve the MEMS switch's response time, the spring constant of the beam should be increased, and besides, the thickness of the beam should be decreased.

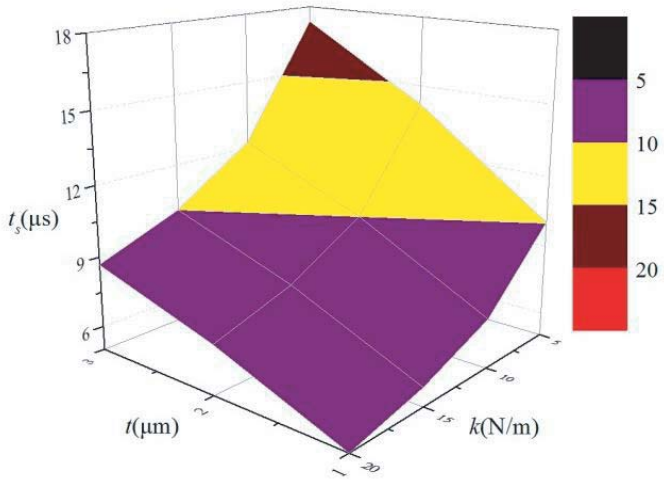

Figure 4. The relationship among the thickness, the spring constant and the switching time.

The structure of the beam is as shown in Fig. 5. The anchor with the arc structure and the square holes with a size of 10 μm × 10 μm in the beam are to release the residual stress [20]. The anchors are located at the ends of the fixed-fixed beam.

2.2. Simulation and Optimization of the RF MEMS Switch Electronic Properties

Nowadays, various beam structures have been reported, to improve the mechanical performance of MEMS switches. Meanwhile, several transmission line structures, such as short stubs, have been used in MEMS switches, to realize high isolation for specific frequency band. Discontinuous CPW ground can realize the frequency tuning for the microwave device based on CPW transmission line, so the structure has been used in MEMS switch [19], MEMS filter [17], and MEMS antenna.

RF MEMS capacitive switch has an obvious feature, which is a dielectric layer used in the capacitive switch. From the capacitive shunt switch equivalent circuit in Fig. 6, it can be found that the impendence of MEMS beam is less than the port characteristic impedance Z. In order to realize impedance matching, some approaches have been reported (such as "T" circuit) [6]. In Fig. 6, $Z_1(\beta l)$ represents the line to realize impedance matching of the switch, and $Z_b(\beta l_b)$ represents the MEMS switch's characteristic impedance.

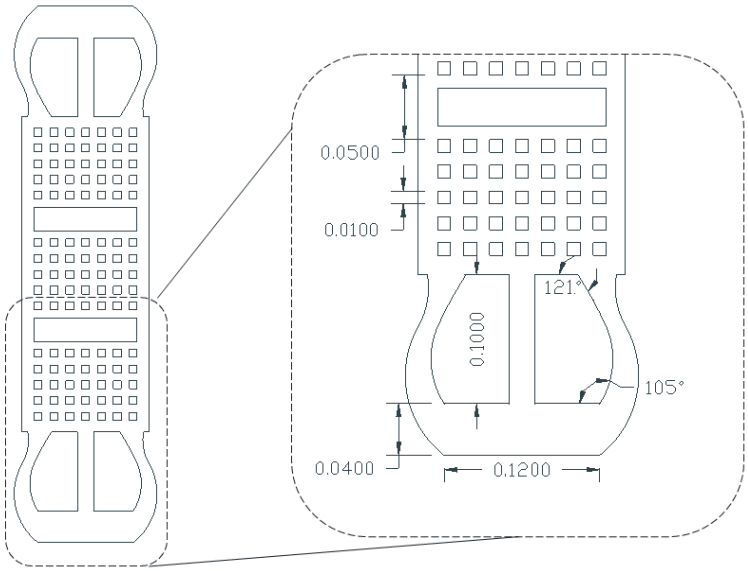

Figure 5. The structure of the fixed-fixed beam.

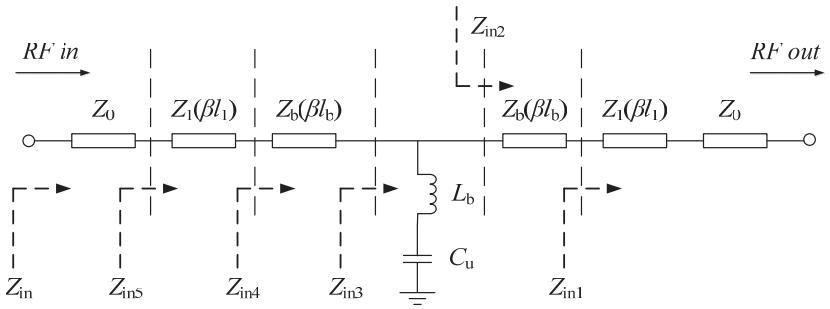

Figure 6. The equivalent circuit of the MEMS capacitive switch.

These circuit parameters in Fig. 6 can be calculated by the formulas as follows [21].

$$Z_{in1} = Z_1 \frac{Z_0 + jZ_1 \tan \beta l_1}{Z_1 + jZ_0 \tan \beta l_1}; \quad Z_{in2} = Z_b \frac{Z_{in1} + jZ_b \tan \beta l_b}{Z_b + jZ_{in1} \tan \beta l_b}; \quad Z_{in3} = \frac{Z_{in2}\left(j\omega L_b + \dfrac{1}{j\omega C_u}\right)}{Z_{in2} + \left(j\omega L_b + \dfrac{1}{j\omega C_u}\right)} \tag{11}$$

$$Z_{in4} = Z_b \frac{Z_{in3} + jZ_b \tan \beta l_b}{Z_b + jZ_{in3} \tan \beta l_b}; \quad Z_{in5} = Z_b \frac{Z_{in4} + jZ_1 \tan \beta l_1}{Z_1 + jZ_{in4} \tan \beta l_1}; \quad Z_{in} = Z_0 \frac{Z_{in5} + jZ_0}{Z_0 + jZ_{in5}}$$

For K-band MEMS switches, in order to calculate the parameters easier, it is assumed that the central frequency of MEMS switch is 20 GHz, and the parameters of the circuit in Fig. 6 are defined in Table 1. From above formulas, the value of Z_1 is $138.1 + 229.8i$.

Table 1. The parameters of the circuit in Fig. 6.

para	value	para	value	para	value
Z_0	50 Ω	Z_b	30 Ω	L_u	30 pH
C_u	30 fF	f	20 GHz	l_1	0.2 mm
l_b	0.3 mm	ε_r	11.9	Z_1	$138.1 + 229.8i$

For the "T" circuit, two high impedance transmission lines are connected to the MEMS switch, respectively [6]. The high impedance transmission of CPW lines can be realized by two ways. One way is to decrease the width of CPW signal line, and the other way is to decrease the gap between the ground and the signal.

As show in Fig. 7, the actuation poles and CPW transmission line are located at the bottom of the MEMS beam, and they are covered with the dielectric layer of SiN. As known, compared with cantilever beam, the spring constant of fixed-fixed beam is higher, so the actuation voltage of the fixed-fixed beam is larger. To improve the switching time, the actuation voltage of the RF MEMS switch cannot be too low, such as the voltage of the ADI Corporation's MEMS switch being 80 V. However, when the actuation voltage of the MEMS switch with dielectric layer of 0.15 µm-thickness is more than 30 V, it will cause the phenomenon of dielectric charge to decrease the lifetime of the switch. To avoid the proposed MEMS switch contact to the actuation poles when the switch is pulled down, the thickness of poles is less than CPW transmission line in this design. When the MEMS switch is loaded with the DC voltage, the beam is pulled in to contact with the CPW signal line and keep a distance from the poles.

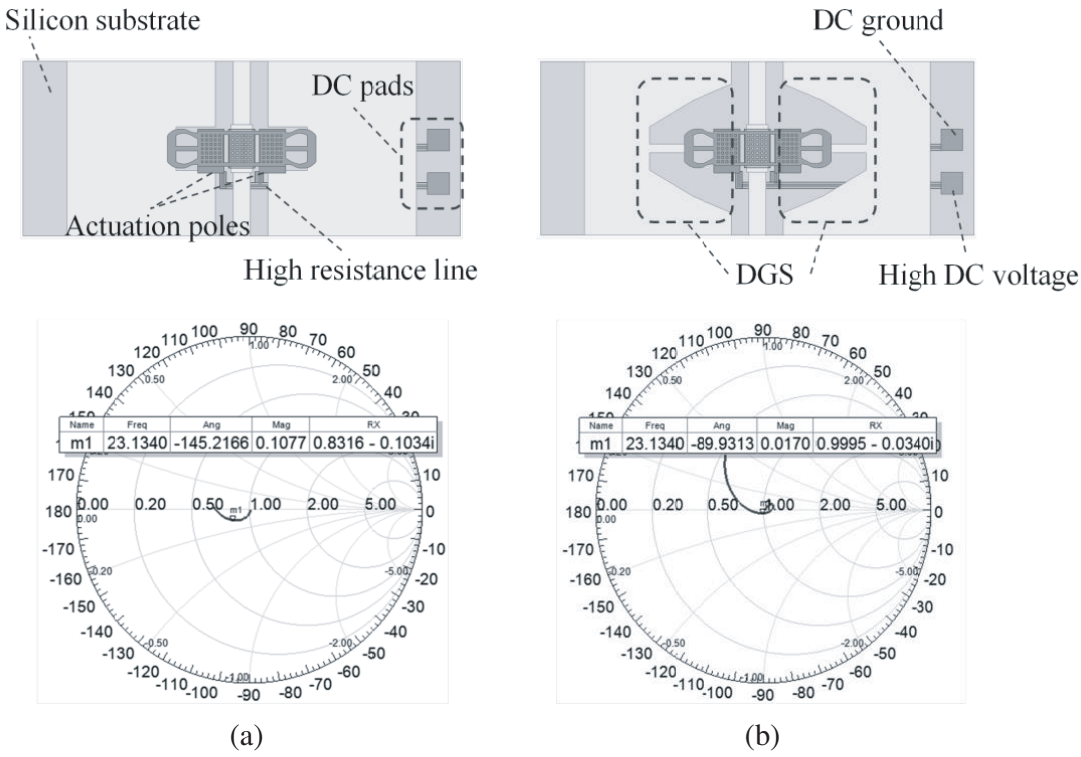

Figure 7. Simulated smith chart of the RF MEMS switch with different structures.

Two MEMS switches based on different CPW structures are modeled, and the S parameters' performances of the MEMS switches are simulated by HFSS software, which are as shown in Fig. 7. The structure of the MEMS switch with the rectangle DGS and its simulated smith chart are given in Fig. 7(a). The characteristic impedance of the MEMS switch in K-band is mismatched with the port impedance. The input characteristic impedance Z_{in} of the MEMS switch is $(0.8316 - 0.1034i) \times 50\,\Omega$. From Formula (11), it is shown that Z_{in} is capacitive and that the real part impedance Z_b of the beam is relatively small. In order to increase the real part impedance and reduce the capacitive impedance, DGS with a relatively large size is designed. With the size of DGS increasing, the impedance of the transmission line is increased because the capacitance between signal and ground is reduced. The structure can improve the agreement between the MEMS switch's characteristic impedance and the port impedance. From the simulated Smith chart in Fig. 7(b), the MEMS switch's reflection coefficient is neatly zero, which means that DGS improves the MEMS switch's VSWR.

3. FABRICATION

This proposed MEMS switch is fabricated on the high resistivity silicon with a thickness of 400 µm. A layer of SiO_2 is located on top of the silicon substrate. A layer of SiCr is as the high resistivity line, which is used to decrease the collision energy when the MEMS switch is pulled down [6]. Deposition and partition of a layer of SiN are realized by plasma enhanced chemical vapor deposition (PECVD), and the dielectric layer is to prevent short circuit between the high resistivity and CPW signal. Au is sputtered and electroplated to form the CPW transmission line. As the MEMS capacitive switch's dielectric layer, SiN is PECVD again. The polyimide is as the sacrifice layer, and it is removed by supercritical dry release. Au is sputtered and electroplated, and it is as the material of bridge layer. The microscope of the fabricated MEMS switch is as shown in Fig. 8. The two GSG microwave probes are used to measure the MEMS switch.

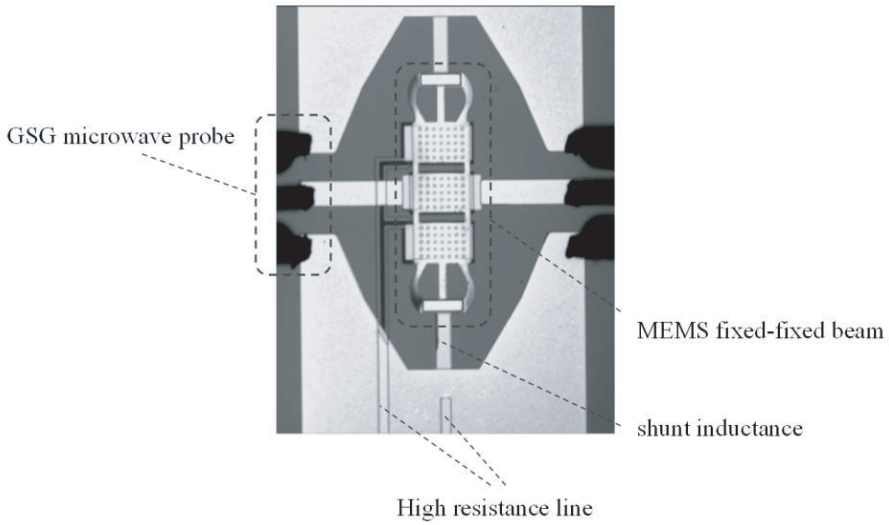

Figure 8. The microscope image of the fabricated MEMS capacitive shunt switch.

4. MEASUREMENT AND ANALYSIS

4.1. *S* Parameter and Actuation Voltage of RF MEMS Switch

The insertion loss, isolation, and return loss of the RF MEMS switch are measured, and the results are obtained by cascade probe station, vector network analyzer. The measured results are illustrated in Fig. 9. The isolation in the K-band is more than 17 dB, the insertion loss better than 0.49 dB, and the return loss better than 22 dB. From Fig. 9(d), the off-state of the switch is formed because of the reflection of the MEMS switch in K-band, and vice versa.

4.2. Switching Time of This Proposed Switch

The RF MEMS switch is measured by cascade probe station, detector, function generator, and oscilloscope to obtain the on/off time. The circuit diagram of the measured system for the proposed RF MEMS switch is as shown in Fig. 10. The measured results of on/off time are as shown in Fig. 11. The green solid line represents the MEMS switch's RF out power detected by detector, and the blue solid line represents the square wave DC bias voltage for the MEMS switch. When the MEMS switch is actuated by a voltage of 54 V, the switch is pulled down to contact with the dielectric layer, and it changes the on-state to the off-state. The switching time is 54 µs. On the contrary, when the pull-in voltage is 0 V, the fixed-fixed beam is released, and the MEMS switch changes its off-state to the on-state. The switching time is 168 µs.

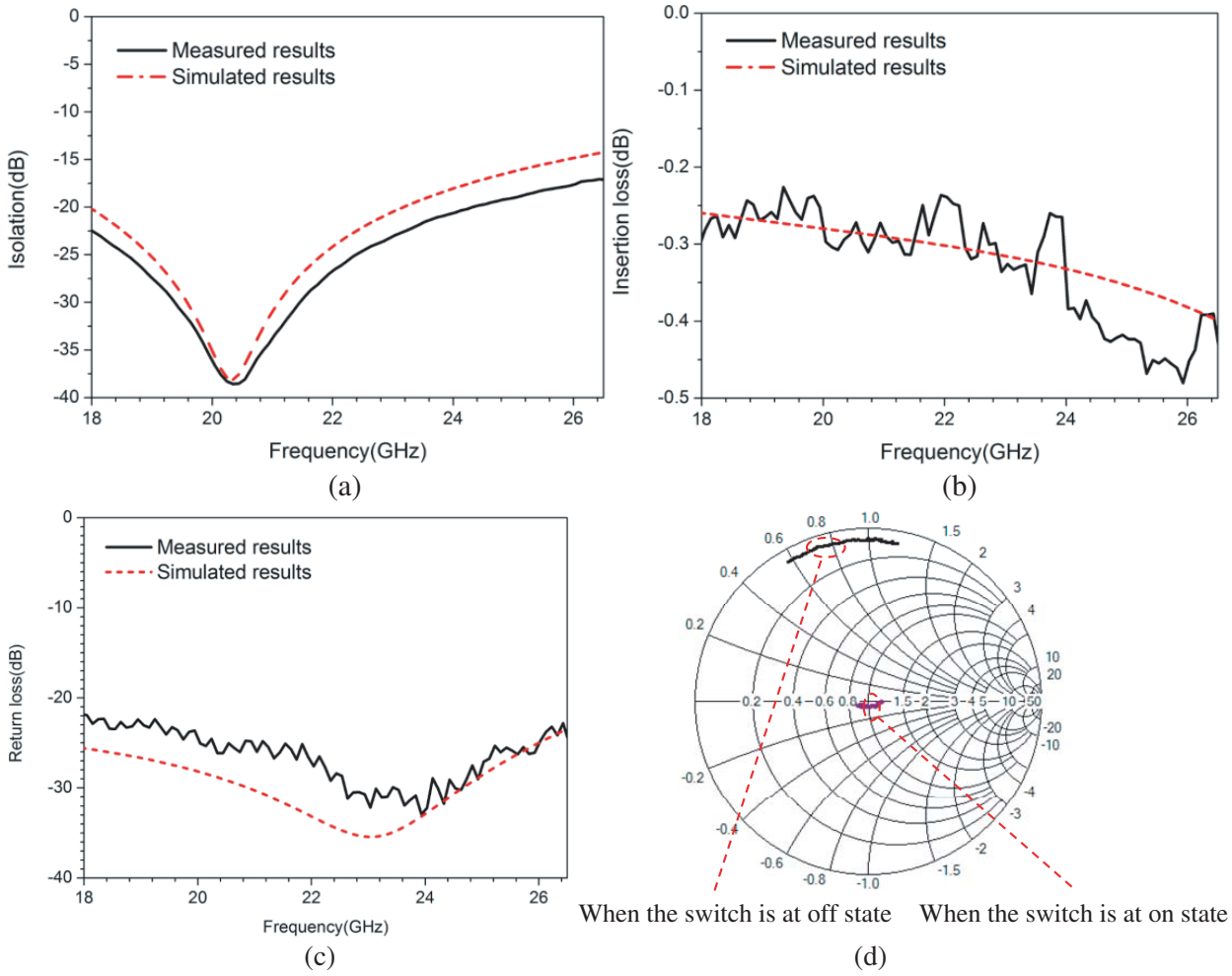

Figure 9. The measured S parameters results of the proposed MEMS switch.

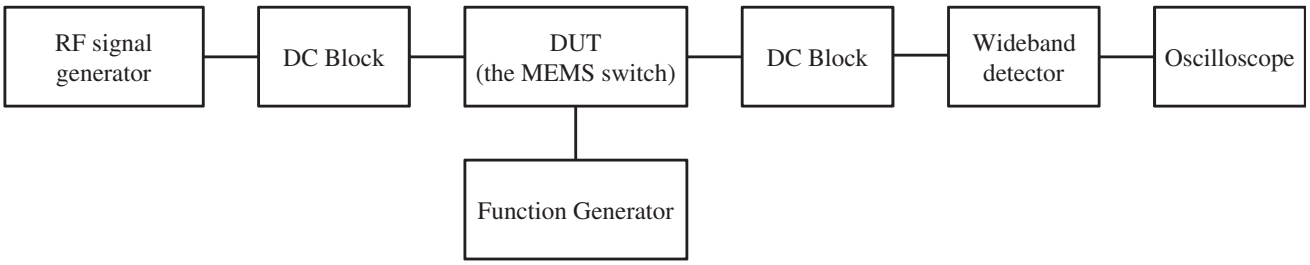

Figure 10. The circuit diagram of the measured system for the proposed RF MEMS switch.

4.3. Analysis of the Measured Results

As illustrated in Fig. 9, the simulated results by HFSS are represented by dotted lines, and the measured results are represented by solid lines. For K-band, comparison between the simulated and measured results is at good agreement.

From Table 2, the switch proposed by this work exhibits with a comprehensive performance, and it has a better switching time especially. The insertion loss of this proposed MEMS switch is better than other K-band MEMS switches with measurement, and the return loss and isolation are also good.

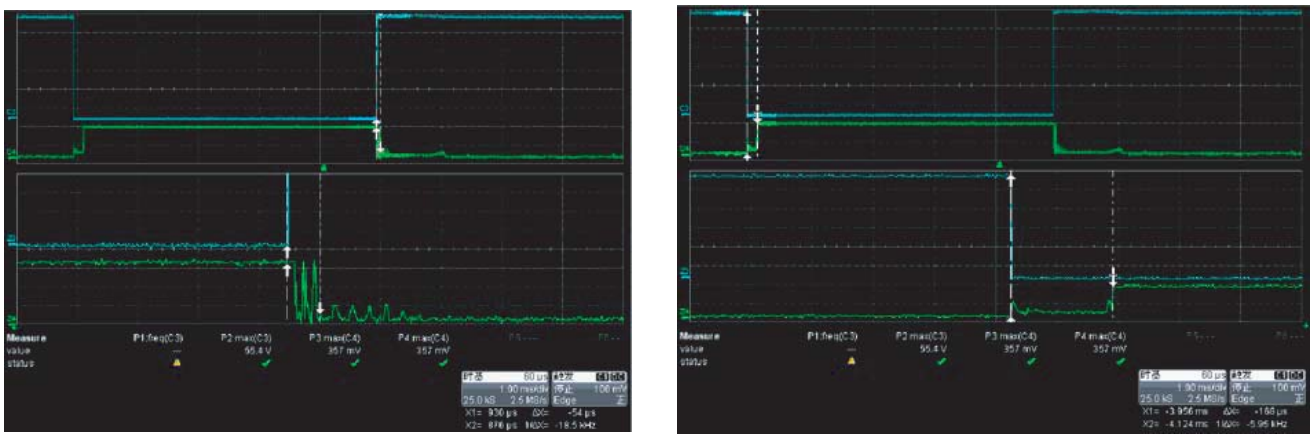

(a) (b)

Figure 11. The measured on/off time of the proposed RF MEMS switch.

Table 2. Compared with other K-band RF MEMS switch.

Reference	Retrun loss	Insertion loss	Isolation	Actuation	pull-in/release Switching time
[12]	NA	0.8 dB @25 GHz	20 dB @25 GHz	25 ∼ 40 V of voltage	100 µs (release)
[14]	< -10 dB @20 GHz	< 1 dB @20 GHz	11 dB @20 GHz	55 V of voltage	55 µs@65 V 20 µs (release)
[15]	< -22 dB @26 GHz	0.6 dB @26 GHz	> 20 dB @26 GHz	250 mW@ Hot-actuation	14 ms/∼ 3 ms
[16]	NA	≤ 1 dB @K-band	≥ 23 dB @K-band	34 V of voltage	NA
[17]	< -30 dB @K-band Only simulated	≤ 0.1 dB @K-band Only simulated	≥ 13 dB @K-band Only simulated	20 V of voltag Only simulated	NA
[18]	< -26.27 dB@ 25 GHz Only simulated	0.11 dB@ 25 GHz Only simulated	52 dB @10 GHz Only simulated	11.75 V Only simulated	56.41 µs Only simulated
[22]	NA	0.5 ∼ 1 dB @15 ∼ 25 GHz	16 ∼ 20 dB @15 ∼ 25 GHz	30 V	NA
[23]	NA	1.1 dB 20 GHz	35 dB @20 GHz	20 V	NA
This work	< -22 dB @K-band	< 0.5 dB @K-band	> 17 dB @K-band	54 V of voltage	54/168 µs

*NA = Not Available

5. CONCLUSION

It is a trend that the communication system's operating frequency becomes higher and higher. The MEMS switch exhibits low insertion loss and low power consumption. For K-band communication application, a novel switch using MEMS technology is designed, simulated, fabricated, and measured. In order to improve the RF performance of the switch, DCPW structure is designed and used to the MEMS switch. The performance of the insertion loss, isolation, actuation voltage, and switching time of the proposed MEMS switch are all measured. The agreement between the measured and simulated results is good. This proposed MEMS switch exhibits lower insertion loss than other K-band MEMS switches.

REFERENCES

1. Watson, T., S. Miller, D. Kershner, and G. A. Anzic, "Design of a K-band transmit phased array for low Earth orbit satellite communications," *Proceedings 2000 IEEE International Conference on Phased Array Systems and Technology (Cat. No. 00TH8510)*, 211–214, Dana Point, CA, 2000.
2. Dey, S. and S. K. Koul, "Reliability analysis of Ku-band 5-bit phase shifters using MEMS SP4T and SPDT switches," *IEEE Trans. Microwave Theory Tech.*, Vol. 63, No. 12, 3997–4012, Dec. 2015.
3. Tahir, F. A., H. Aubert, and E. Girard, "Equivalent electrical circuit for designing MEMS-controlled reflectarray phase shifters," *Progress In Electromagnetics Research*, Vol. 100, 1–12, 2010.
4. Daneshmand, M. and R. R. Mansour, "RF MEMS satellite switch matrices," *IEEE Microw. Mag.*, Vol. 12, No. 5, 92–109, Aug. 2011.
5. Jia, S. and F. Zhao, "Design of a MEMS reconfigurable group delay equalizer," *Radio Engineering*, Vol. 48, No. 4, 208–313, 2018.
6. Rebeiz, G. M., *RF MEMS Theory, Design, and Technology*, John Wiley & Sons, 2004.
7. Khalichi, B., S. Nikmehr, and A. Pourziad, "Reconfigurable SIW antenna based on RF MEMS switches," *Progress In Electromagnetics Research*, Vol. 142, 189–205, 2013.
8. Pourziad, A., S. Nikmehr, and H. Veladi, "A novel multi-state integrated RF MEMS switch for reconfigurable antennas applications," *Progress In Electromagnetics Research*, Vol. 139, 389–406, 2013.
9. Martinez-Lopez, R., J. Rodriguez-Cuevas, A. E. Martynyuk, and J. I. Martinez-Lopez, "An active ring slot with RF MEMS switchable radial stubs for reconfigurable frequency selective surface applications," *Progress In Electromagnetics Research*, Vol. 128, 419–440, 2012.
10. Carty, E., P. Fitzgerald, P. McDaid, B. Stenson, and R. Goggin, "Development of a DC to K-band ultra long on-life RF MEMS switch with integrated driver circuitry," *2016 46th European Microwave Conference (EuMC)*, 1373–1376, London, 2016.
11. Topalli, K., M. Unlu, H. I. Atasoy, S. Demir, O. A. Civi, and T. Akin, "Empirical formulation of bridge inductance in inductively tuned RF MEMS shunt switches," *Progress In Electromagnetics Research*, Vol. 97, 343–356, 2009.
12. Persano, A., A. Tazzoli, P. Farinelli, et al., "K-band capacitive MEMS switches on GaAs substrate: Design, fabrication, and reliability," *Microelectron Reliab*, Vol. 52, Nos. 9–10, 2245–2249, 2012.
13. Cohn, M. B., K. Saechao, M. Whitlock, et al., "RF MEMS switches for wide I/O data bus applications," *2013 IEEE International Test Conference (ITC)*, 1–8, 2013.
14. Yang, H. H., H. Zareie, and G. M. Rebeiz, "A high power stress-gradient resilient RF MEMS capacitive switch," *J. Microelectromech Syst.*, Vol. 24, No. 3, 599–607, 2015.
15. Bakri-Kassem, M. and R. R. Mansour, "High power latching RF MEMS switches," *IEEE Trans. Microwave Theory Tech.*, Vol. 63, No. 1, 222–232, 2015.
16. Carty, E., P. Fitzgerald, P. McDaid, B. Stenson, and R. Goggin, "Development of a DC to K-band ultra long on-life RF MEMS switch with integrated driver circuitry," *2016 46th European Microwave Conference (EuMC)*, 1373–1376, London, 2016.
17. Hamad, E. K. I., A. M. E. Safwat, and A. S. Omar, "A MEMS reconfigurable DGS resonator for K-band applications," *J. Microelectromech Syst.*, Vol. 15, No. 4, 756–762, Aug. 2006.

18. Angira, M. and K. Rangra, "Design and investigation of a low insertion loss, broadband, enhanced self and hold down power RF-MEMS switch," *Microsyst. Technol.*, Vol. 21, No. 6, 1173–1178, 2015.
19. Zareie, H. and G. M. Rebeiz, "High power (> 10 W) RF MEMS switched capacitors," *2012 IEEE/MTT-S International Microwave Symposium Digest*, 1–3, 2012.
20. Wei, H., Z. Deng, X. Guo, Y. Wang, and H. Yang, "High on/off capacitance ratio RF MEMS capacitive switches," *J. Micromech. Microeng.*, Vol. 27, 055002, 2017.
21. Pozar, D. M., *Microwave Engineering*, John Wiley & Sons, 2009.
22. Malmqvist, R., C. Samuelsson, A. Gustafsson, H. Maher, T. Vähä-Heikkilä, and R. Baggen, "A K-band single-chip reconfigurable/multi-functional RF-MEMS switched dual-LNA MMIC," *2012 IEEE/MTT-S International Microwave Symposium Digest*, 1–3, Montreal, QC, 2012.
23. Puyal, V., D. Dragomirescu, C. Villeneuve, J. Ruan, P. Pons, and R. Plana, "Frequency scalable model for MEMS capacitive shunt switches at millimeter-wave frequencies," *IEEE Trans. Microwave Theory Tech.*, Vol. 57, No. 11, 2824–2833, Nov. 2009.